FORUM GEOGRAFI
ISSN: 0852-0682 | E-ISSN: 2460-3945
HTTPS://JOURNALS.UMS.AC.ID/INDEX.PHP/FG/

Research article

Volcanic Pumice Rafts at Sea: Buoyancy and Infiltration with Micro-particles

Sawada Sho[1,*], Gomez Christopher[1], Koi Takashi[2]

[1] Kobe University, Laboratory of Sediment Hazards and Disaster Risks (SABO) at the Faculty of Oceanology, Higash-inadaku Fukaeminamimachi 5-1-1, Kobe City, Japan; [2] Center for Natural Hazards Research, Hokkaido University Kita 9 Nishi 9 Kita-Ku, Sapporo, Hokkaido 060-8589, Japan

[*)] Correspondence: 232w315w@stu.kobe-u.ac.jp

Citation:
Sho, S., Christopher, G., Takashi, K. (2025). Volcanic Pumice Rafts at Sea: Buoyancy and Infiltration with Micro-particles. Forum Geografi. 39(1), 53-63.

Article history:
Received: 2 December 2024
Revised: 23 January 2025
Accepted: 27 January 2025
Published: 15 March 2025

Abstract

Pumice, characterised by its high vesicularity, often forms pumice rafts as it floats on water. Although the vast majority of research has focused on understanding the behavior of pumice rafts, studies on the water infiltration properties of pumice remain scarce. Moreover, the influence of underwater particles, such as microplastics in the ocean, on water infiltration through the pores of pumiceous materials is still unclear. Therefore, this study investigates the water infiltration properties of pumice mate-rials and their behavior in different aqueous environments through laboratory experiments using pumiceous rocks (En-a, originating from Mount Eniwa) from the 2018 Hokkaido Eastern Iburi earthquake site. Experiments were conducted in both still and slurry water conditions to examine the effects of particle size and sediment concentration on water infiltration rates. Results showed that density variations follow a two-phase pattern: a rapid initial increase (+0.43 g/cm³ and 0.3931 g/cm³ in the first 30s for small and large pumice, respectively) followed by a plateau phase (+0.022 g/cm³ and 0.0197 g/cm³ in the next 60s). Statistical analysis revealed significant differences in infiltration rates based on particle size in still water conditions, with smaller pumices showing more heterogeneous infiltration pathways. While sediment presence in slurry conditions did not significantly affect overall infiltration rates, it led to more stable data dispersion, particularly in larger samples. The study also pro-poses a statistical framework for modeling pumice behavior, incorporating parameters such as vesicularity, particle concentration, and temperature. These findings suggest that current pumice raft models need refinement to account for size-dependent infiltration behaviors and the influence of underwater particles, with implications for understanding the transport and environmental impact of pumice rafts in marine environments.

Keywords: Pumice; Pumice Rafts; Ocean Wastes; Marine Ecosystems.

1. Introduction

1.1. Conceptual Background

This chapter outlines the background adequately. Research problem should be elaborated with short review of literature and previous related publications. Authors are required to include the citation of the previous published article from reputable journals. Describe the purposes of the research to complete this part. Pumice, characterized by its high vesicularity, remains buoyant on water and often forms extensive “pumice rafts”, resulting from massive amount of pumice discharged by volcanic eruptions within the ring of fire and from submarine volcanoes. While the distribution within the ring of fire can lead to the pumice generation on the ocean, the investigations of underwater volcanic events remain scarce. (Figure 1, Table 1). While they can influence alter ecosystems including coral reefs and mangroves (Ohno *et al.*, 2022)., pumice rafts can, in turn, facilitate the spread of marine organisms, such as algae and bacteria, and particles in the ocean. In particular, pumice contemporarily reduce the concentration of micro plastics (MPs) on the ocean surface by capturing them through its pores. However, the MPs entrapped in its porous structures can be reintroduced into the ocean environment due to its fragments, in the long run. (Pradit *et al.*, 2022). The MPs retained within pumice may potentially serve as geological markers of the Anthropocene in the future, and these complexities are likely to be preserved in stratigraphic layers, characterizing the Anthropocene epoch (Majcen *et al.*, 2024; Woodroffe & Stancheva, 2024; Yin *et al.*, 2024). During volcanic eruptions, meanwhile, volcanic ash is also ejected alongside pumice. Vol-canic ash can be produced in the process of pumice rafts, undergoing collision, friction, and chemical dissolution, influenced by ocean currents and wind, due to the exposure to saline seawater containing trace elements (Jutzeler *et al.*, 2014), after which they disperse widely as fine particles in the ocean via thermal convection and density currents, akin to MPs. (Murch *et al.*, 2019, 2020).

Volcanic eruptions can affect both coastal habitats and human environments. For instance, a total of 33 cases of volcanic ash-induced engine damage caused by volcanic ash encounters were reported (Christmann *et al.*, 2017). Most of these incidents occurred in the Ring of Fire, including Southeast Asia, New Zealand, North America, and Europe (especially around Iceland) (Christmann *et al.*, 2017), and the primary causes were a) ash particles melting within the engine and

recrystallizing on turbine blades b) clogging of air intake filters by ash, limiting the engine's air supply, and c) high-temperature ash leading to physical abrasion or corrosion of turbine components (Casadevall, 1993; Prata and Rose, 2015; Christmann *et al.*, 2017). Research has focused on establishing volcanic ash concentration standards and improving ash cloud prediction models to mitigate these risks (e.g. Casadevall, 1993; Whitham *et al.*, 2012; Prata and Rose, 2015; Christmann *et al.*, 2017). Also, Skid resistance on road asphalt and runway concrete is notably reduced by volcanic ash, especially when the ash is rhyolitic or when conditions are wet. Given that the rafts can affect both coastal habitats and maritime navigation, on the other hand, the prompt necessity for timely tracking and prediction methods has been pointed out (Jutzeler *et al.*, 2014). Laboratory flow-tank experiments indicate that pumice movement is constrained by channel width, with wider pathways facilitating smoother flow, while narrow areas cause the accumulation (Nagayama & Izaki, 2022). On the other hand, pumice behaviour in aquatic environments has unique cooling properties. Slowly cooling underwater pumice retains the buoyancy of its internal bubbles (Von Lichtan *et al.*, 2016). Furthermore, the proportion of floating pumice varies depending on the eruption: the 2019 Havre event, for instance, produced over 90% floating pumice, whereas 30 to 70% for the eruption of Volcano-F in 2019, suggesting that eruption dynamics and vent location may play critical roles in the distribution (Yeo *et al.*, 2024).

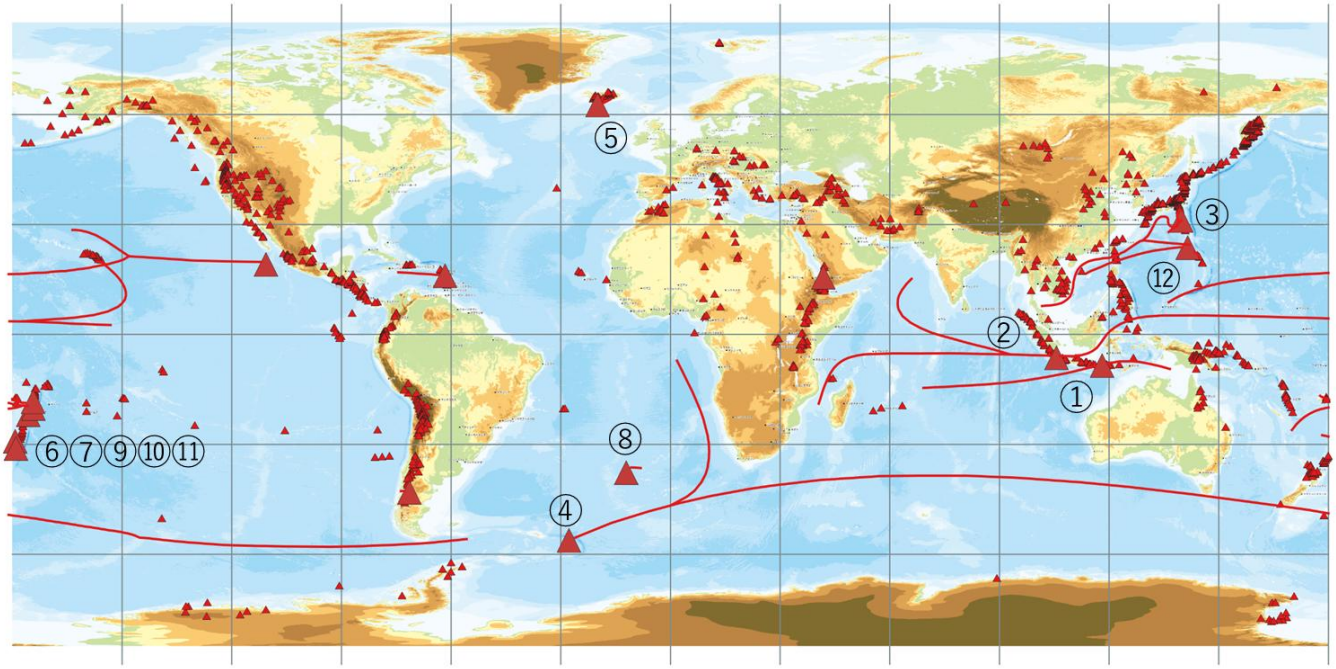

Figure 1. Representative Pumice Rafting Events. Red Triangles: the Location of Volcanoes (The Source Of Pumice Rafts with a Larger Triangle); Red Lines: The General Trajectory Paths of Pumice Rafts (After Bryan *et al.*, 2004). Note: the Trajectory Data Source for ⑩ is Missing.

Table 1. Representative Pumice Rafting Events Over the Last 200 Years.

Dates	Eruptions	Region	Location	References
1815	Tambora	Indonesia	①	Oppenheimer (2003)
1883	Krakatau	Indonesia	②	Jokiel and Cox (2003)
1952-1953	Myojinsho	Japan	③	Fiscke *et al.* (1998)
1962	South Sandwich Islands	British overseas territory	④	Sutherland (1965); Risso *et al.* (2002)
1962	Surtsey	Iceland	⑤	Gudmundsson and Ingolfsson (1967)
1964	(Unknown)	Tonga	⑥	Bryan (1968)
2001	0403-091	Tonga	⑦	Bryan *et al.* (2004)
2004	Tristan de Cunha	British overseas territory	⑧	Reagan *et al.* (2008)
2006	Home Reef	Tonga	⑨	Vaughan *et al.* (2007)
2012	Havre Seamount	Kermadec Arc	⑩	Jutzeler *et al.* (2014)
2019	0403-091	Tonga	⑪	Redick (2023); Yeo *et al.* (2024)
2021	Fukutoku-okanoba	Japan	⑫	Maeno *et al.* (2022); Yoshida *et al.* (2022)

1.2. Water Infiltration Properties of Pumice Materials

Pumice absorption, with two different infiltration phases, can be simplified as Fourier's Law (Equation 1), mathematically similar to diffusion laws (Manville *et al.*, 1998):

$$\mathbf{Q}^* = -\mathbf{K}^*\mathbf{A}\frac{\boldsymbol{\delta}\mathbf{T}}{\boldsymbol{\delta}\mathbf{x}} \quad (1)$$

Where Q^* is the heat flux through the cross-sectional area A, δT is the temperature difference across the distance δx, and K^* is the thermal conductivity. In the initial phase, water rapidly infiltrates the surface and outer vesicles. Over time, however, the absorption rate decreases as water penetrates deeper, ultimately reaching saturation. This delayed absorption can be explained by the differences in water absorption rates between the outer layer and the internal structure (Whitham and Sparks, 1986; Manville *et al.*, 1998, 2002).

The time required for pumice to sink (tsink) is highly dependent on pumice size and vesicle characteristics. Manville *et al.* (1998) have revealed that the tsink is proportional to the square of the pumice's radius, smaller clasts sinking more quickly due to faster water infiltration, while larger pumices remain afloat longer (Manville *et al.*, 1998).

Resin-based analysis has also shown that interconnected vesicles facilitate water infiltration and air escape, leading to sinking (Whitham and Sparks, 1986). Moreover, temperature also influences sinking; high-temperature pumice generates steam, rapidly expelling air from vesicles and causing immediate sinking, with a threshold of temperature varying depending on the density, suggesting that even low-density pumice can sink when sufficiently heated (Whitham and Sparks, 1986).

While the vast majority of research has worked on revealing the behaviour of pumice rafts, the investigations into the water infiltration of pumice are very limited. Also, the effect of underwater particles (such as microplastics in the ocean) on the water infiltration of pumiceous materials has yet to be known. Therefore, the authors aim to clarify the role of the material density of underwater pumice and particles in the vesicles on the water infiltration and the behaviour of pumice rafts. The investigation of the water infiltration itself and the effect of particles on the water infiltration can contribute to clarify the sinking process (Whitham and Sparks, 1986), leading to the modelling of the behaviour of pumice rafts accounting for the infiltration variation.

2. Research Methods

2.1. Materials

The present research relies on a set of laboratory experiments using the pumiceous rocks of the slope that collapsed during the 2018 Hokkaido Eastern Iburi earthquake in northern Japan. In total, 343 blocks of pumice were used for each repeat of experiments (Figure 2).

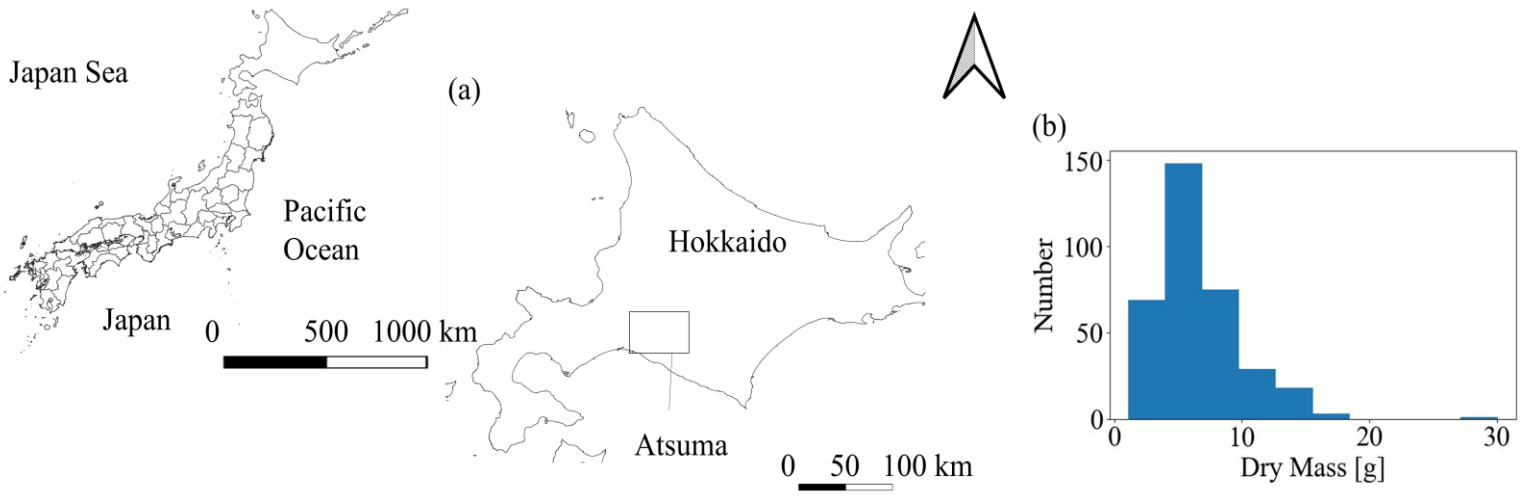

Figure 2. Distribution of All Samples (a) and the Samples from Each Region (b).

2.1. Methods

The method of the experiments is divided into two different settings: a first one with still water, the second one was tested in slurry water with sediment, which is expected that the sediment should deter the water infiltration into a pumice (Table 2).

Table 2. The Samples Used in This Laboratory Experiment, and Details of the Experiment About the Period of Time, Water Speed Type, Scale Used in This Experiment, and the Pumice Conditions.

Period of time	30 seconds ×3 sets for each
Sediment concentration	0, $\frac{5}{400}$ (slurry)
And the diameter	<125μm
Scale	0.1g HL-200i

First group of experiments: the pumices were first sunk in a water bath at air temperature ("still" water) using a tweezer to limit the contact between any manipulation instrument and the sample surface. The sediment mass-change due to water infiltration was then measured using a 0.1 g HL-200i scale, with a measurement every 30 seconds for 90-second periods of time. For the second group of experiments, the same time-step as the first was used in "slurry" water with sediment particles (the diameter is <125μm) created from the Iburi samples. Afterwards, the density variation over time in each condition was deduced according to the following procedures (Figure 3).

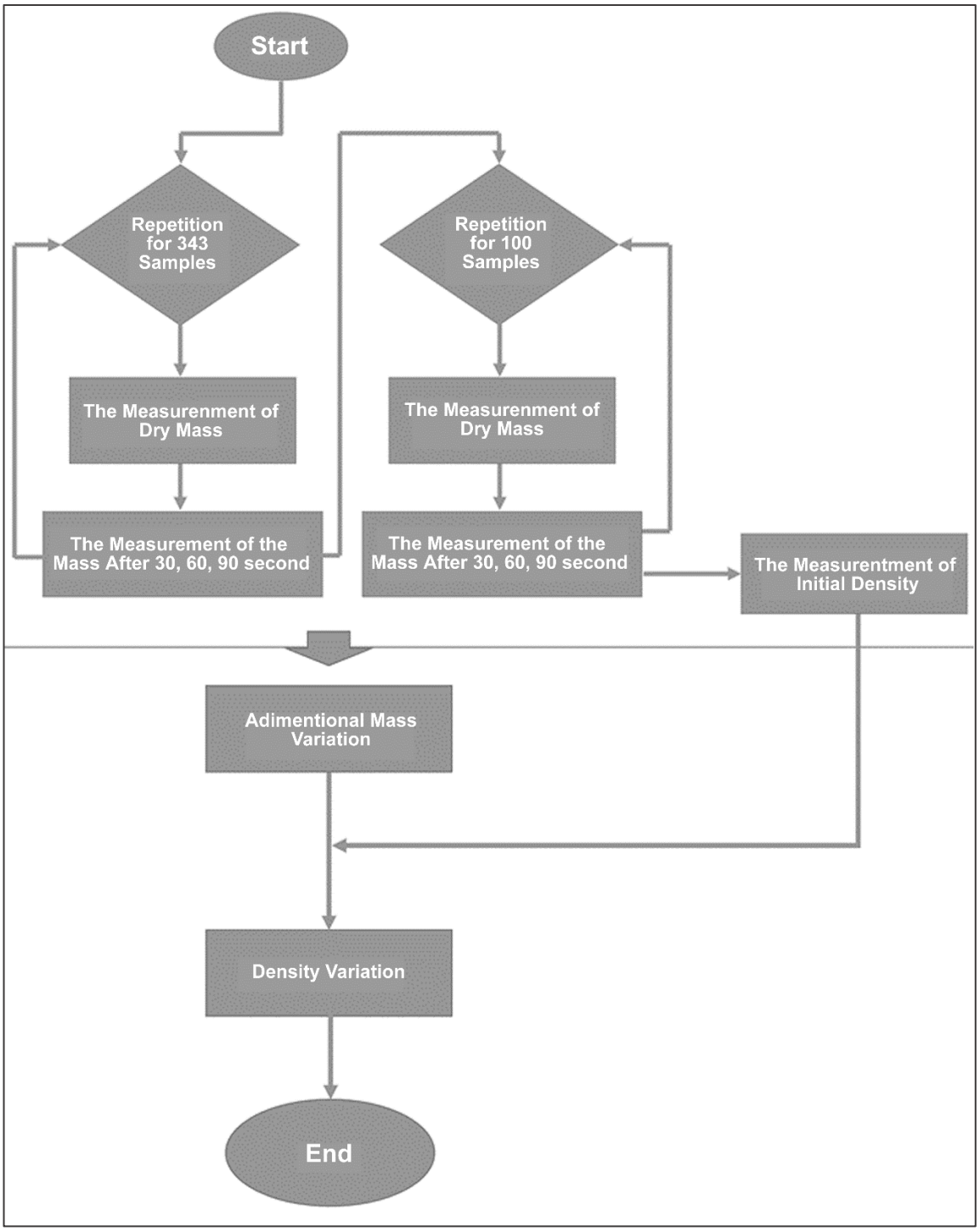

Figure 3. Flow Chart for this Experiment to Gain the Density Variation.

2.1. Measurement of Initial Density

The initial density was determined by the wax coating method (Orosa *et al.*, 2021), and the density for each sample is calculated as Equation 2.

$$\boldsymbol{\sigma(0, x_j) = \frac{m_a}{\frac{m_w}{\rho_w} - \frac{m_d - m_a}{\rho_p}}} \quad (2)$$

where m_a: mass of dry sample in air, m_d: mass of coated specimen in air, m_w: mass of water spilled by coated specimen and ρ_w, ρ_p: specific gravity of water and paraffin. In our contribution, the author dipped the samples into the melted wax to entrapped moisture, and the volume was calculated measuring the mass of water spilled from a silinder filled with water by putting the specimen into it. Also, this set of experiments was conducted at the end of all the procedures lest pores on the samples should be sealed before the experiments completed.

2.1. Calculation of Adimentional Mass Variation to Deduce the Density Variation

The adimentional mass variation is introduced as Equation 3.

$$\boldsymbol{m^*(t_i, x_j) = \frac{m(t_i, x_j)}{m(0, x_j)}} \quad (3)$$

where m^* is adimentional mass [-], varied with time and size. This adimensionalization serves to deduce the density variation, by using the initial density retrieved from Equation 2, owing to the definition of density and its modification as follows:

$$\sigma(t_i, x_j) = \frac{m(t_i, x_j)}{V(x_j)}$$

$$= \frac{m(0, x_j)}{V(x_j)} \frac{m(t_i, x_j)}{m(0, x_j)}$$

$$= \sigma_0 m^*(t_i, x_j) \ (\because \text{Equation 2 and Equation 3})$$

Hence, the density variation along the time and the volume can be expressed as Equation 4.

$$\boldsymbol{\sigma(t_i, x_j) = \sigma_0 m^*(t_i, x_j)} \quad (4)$$

In this contribution, the authors determined the density variation by using the σ_0 as the average of each initial density calculated by (2), and the m^* as the medium of each group of the mass.

2.2.3. Determination of Statistical Significance

Parametric/non-parametric methods in statistic are commonly used to compare the means/medians of two/more than three groups. In this contribution, the data retrieved from each experiment was divided into two depending on the parameter: Large and Small in 'Size' based on the median of all the original masses (5.65 [g]), for each experiment: 'still' and 'slurry', where the threshold of the size was determined as the median of the sample group.

After that, the statistical significance was determined by the Mann-Whitney U and F tests for the difference and variance, because normality could not be confirmed by the results of the p-value of the Shapiro-Wilk test and the Q-Q plot (Figure 4). In this contribution, the significance level α was set to be 5%, and hypothesis of the p-value <0.05 was concluded as the effect is statistically significant rejecting the null hypothesis. The same analysis was conducted even for the dataset of initial density in order to investigate the difference in terms of material density depending on the size.

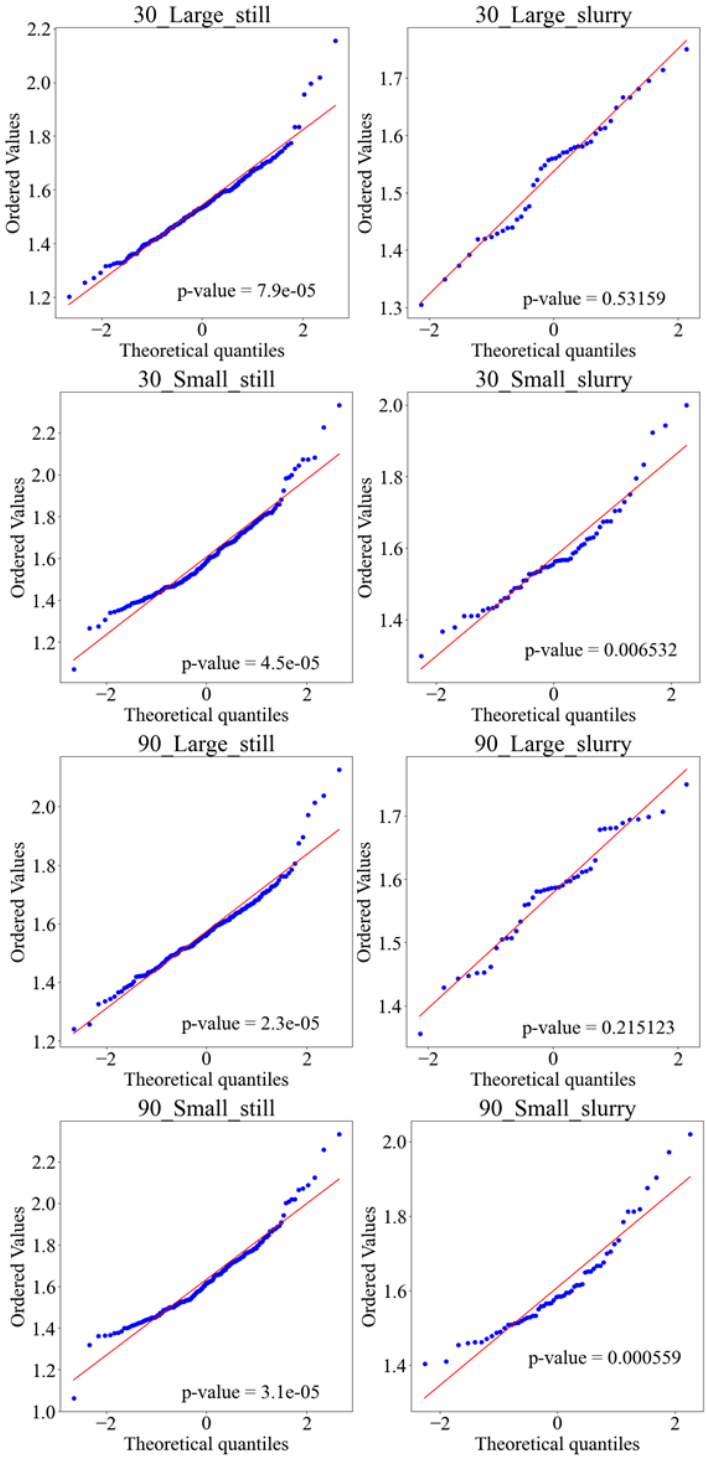

Figure 4. The results of the Shapiro-Wilk test and the Q-Q plot.

3. Results and Discussion

3.1. Adimentional Mass Variation

The result in Figure 5 showed that the median of adimentional mass in every group of the size and water condition increased during 30 and 90 seconds (in still water, 1.58 to 1.61, 1.53 to 1.56 in small/large group of samples, respectively; in slurry water, 1.55 to 1.58, 1.56 to 1.58 in small/large group of samples, respectively). In regards with the differences in size, there is a tendency that the medians are inclined to decrease as the size is larger, although the difference is less significant in slurry water (The difference is 0.052 (30s) and 0.055 (90s), 0.0022 (30s) and 0.0024 (90s) for still/slurry water, respectively). Furthermore, the variance was higher in small group of samples compared to the large (in still water, 0.0203 and 0.0358 (30s), 0.0180 and 0.347 (90s) in large/small group samples, respectively; in slurry water, 0.0109 and 0.0194 at 30s, 0.00810 and 0.0179 at 90s in large/small group samples, respectively). Also, when comparing the same sample

group in each water condition of still and slurry, the difference for the larger group was more significant than the smaller one (in large group, 0.0155 and 0.00948 (30s), 0.0125 and 0.00710 (90s) in still/slurry water, respectively; in smaller samples of group, 0.0178 and 0.0217 (30s), 0.018 and 0.0200 (90s) in still/slurry water, respectively;).

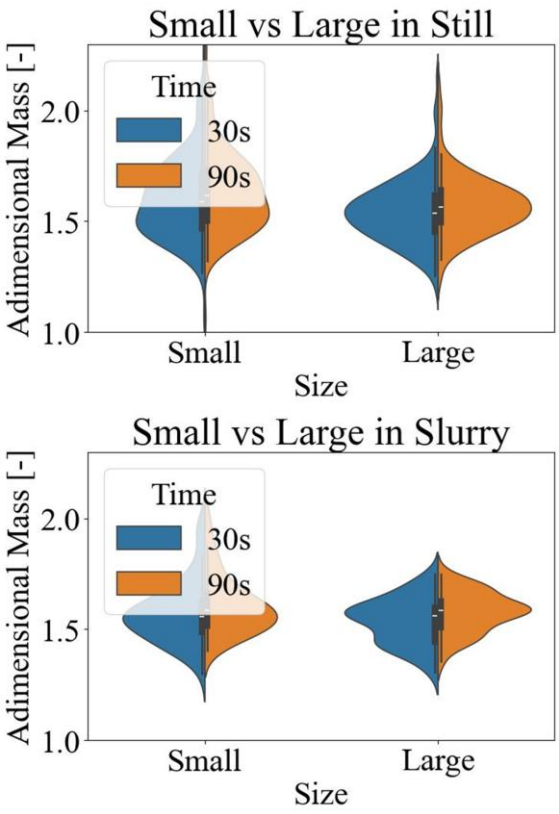

Figure 5. Adimentional mass variation for small/large of samples in still (top) and slurry (bottom) water.

On the other hand, the statistical test was conducted using Mann Whitney-U test, as normality was not confirmed for any classes, with the p-value of the Shapiro-Wilk test showing all < 0.05 except the two classes of large samples in slurry at 30 and 90 seconds, the Q-Q plots for the two classes indicating the deviation from the diagonal line (Figure 4). The results showed that the significant differences were detected mostly in still water for both the changes of time and size, whereas in slurry water, almost no significant differences during the time of 30s to 90s was detected except for large group (Table 3; Table 4). In addition to that, there were no significant differences detected in water condition. Moreover, the results of F test showed that there were significant differences of the variances in size, except in slurry water at 30s. Also, the significant difference of a variance in water condition was detected only in large samples of group in 90s.

Table 3. The results of statistical significance under the significance level of 5% for each group of size, region and water condition for the third round of experiment. CND refers to as the abbreviation of condition. Also, *, **, *** signs were used for different significance levels (p<0.05, p<0.01, p<0.001, respectively).

CND1	CND2	Group	P-Value	Type of Tests
30s	Still	Size	0.00190 **	Mann-Whitney U
90s	Still	Size	0.00261 **	Mann-Whitney U
Small	Still	Time	0.123	Mann-Whitney U
Large	Still	time	0.0258 *	Mann-Whitney U
30s	Slurry	Size	0.111	Mann-Whitney U
90s	Slurry	Size	0.249	Mann-Whitney U
Small	Slurry	Time	0.242	Mann-Whitney U
Large	Slurry	time	0.0237 *	Mann-Whitney U
30s	Large	Water Condition	0.956	Mann-Whitney U
90s	Large	Water Condition	0.551	Mann-Whitney U
Small	Small	Water Condition	0.356	Mann-Whitney U
Large	Small	Water Condition	0.481	Mann-Whitney U

Table 4. The results of statistical significance under the significance level of 5% for each group of size, region and water condition for the third round of experiment. CND refers to as the abbreviation of condition. Also, *, **, *** signs were used for different significance levels (p<0.05, p<0.01, p<0.001, respectively).

CND1	CND2	Group	P-Value	Type of Tests
30s	Still	Size	0.000240 ***	F test
90s	Still	Size	0.0000226 ***	F test
30s	Slurry	Size	0.0549	F test
90s	Slurry	Size	0.00851 **	F test
30s	Large	Water Condition	0.0877	F test
90s	Large	Water Condition	0.0489 *	F test

3.2. Initial Density Regularity among Samples and Density Variation

The result of Figure 6 showed that the initial density of pumice samples: the initial density was determined as 0.734, as the median of a whole group of samples, based on the result that no significant differences in size were detected (p-value was 0.179).

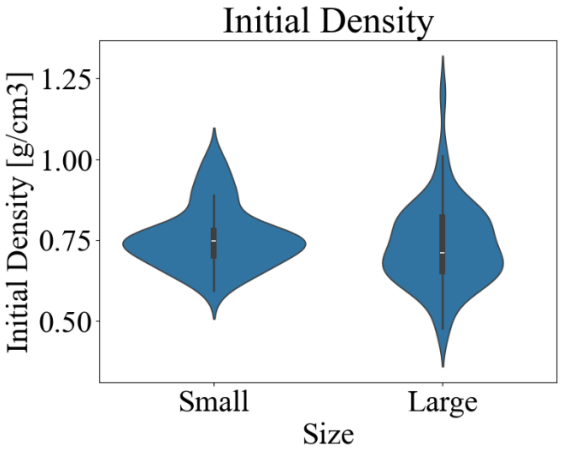

Figure 6. The initial density of the samples.

Equation 5 enabled us to gain the density variation (Figure 7), showing that there are two phases when pumice infiltrates water. The density sharply increased (+0.43, 0.3931 g/cm^3 in the early 30s for small/large pumice) and finally reached the platau (+0.022, 0.0197 g/cm^3 in the next 60s for small/large pumice).

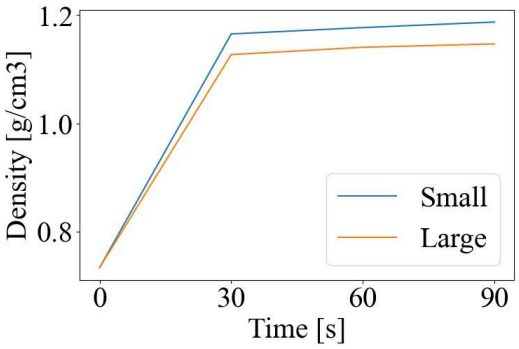

Figure 7. Density variation of the median of each group of dataset against time in still (left) and the slurry (right).

3.3 Discussion

The increasing amount of density over time can be considered due to the water infiltration. However, the behavior varies depending on the effects of the particle size and the water conditions. Water infiltration rates decrease as particle size increases, with smaller pumices reaching their threshold rapidly between 30 and 90 seconds. Moreover, greater dispersion in small group of

samples was revealed as the results of variance analysis, indicating heterogeneous bubble structures that lead to variability in "infiltration pathways". Such variability may derive from blockages within the bubble networks, as mentioned in previous works (e.g. Yu *et al.*, 2023; Zhang *et al.*, 2025), which could lead larger pumices to absorb water with slower yet stable infiltration rates due to consistent bubble structures, while the pathways in smaller pumices are likely to be often blocked, leading to inconsistent infiltration behaviour. Taking the effect of size difference into account, it can be expected that normally, water should be infiltrated into small pumices more rapidly, with the pathways partially deferred due to the blockages, which means that the bubble structures vary depending on the sample, particularly this tendency being likely to be huge in smaller pumices. Therefore, pumice raft models need to be refined with the consideration of the diverse behaviors associated with different size of clasts and inner structures. Specifically, for the larger clasts, they could float and sink over time, as it should need a certain time for the infiltration; on the other hands for the smaller pumices, the clasts could have individual infiltration properties due to different "infiltration pathways".

This experiment detected no significant differences across water conditions. Nonetheless, slurry condition demonstrated more stable data dispersion. In particular, the F test confirmed the significance in water condition towards the large group of samples, along with the results of significant difference that almost no significance was detected for size and time in slurry condition, except for larger samples. One possibility for this is that the data dispersion can be considered due to the dispersion of the "inner pathways to infiltrate", which can be deduced that it is more likely that sediment particles could be either/both excluded in the process of "still" water or/and intrude into the pores in large group of clasts, whereas small group of clasts, with their insufficient pore sizes, may not have allowed the particles intrusion. Either ways, this suggests the influence of particles on the permeability, the current model may not consider this "black-boxed" process, indicating that the model may not be able to be applied when considering the effect of increasing amount of MPs or volcanic ash in the ocean on the infiltration of pumices in a raft.

This study categorised size and sediment concentration (water condition) as Large/Small and Still/Slurry in a binary framework, with significance difference in density variation and its dispersion. However, by rewriting Equation 5 into the form of the probability density function f (Equation 6), the distribution of adimentional mass for each time, size and water condition shown in Figure 5 can be interpreted as "cross-section" of the probability density function f_2 for adimentional mass variation:

$$\mathrm{f} = \mathrm{f}_1(\sigma_0|\mathrm{x}_1, \mathrm{x}_2, \dots) \cdot \mathrm{f}_2(\sigma^*|\mathrm{y}_1, \mathrm{y}_2, \dots) \tag{5}$$

where, f_1, f_2: the probability density functions for original density and adimentional density variation, σ_0, σ^*: original density, adimentional density variation, x_i, y_j $(i, j = 1, 2, \dots)$: the parameters to determine the original density, adimentional density, including the vesicularity and its coalescence, time, diameter of pumices, particle concentration and particle diameter and. In addition, σ^* can be expressed using Equation 5:

$$\sigma^*(t, x) \equiv \frac{\sigma(t, x)}{\sigma_0} = m^*(t, x) \tag{6}$$

Assuming that this study merely treats size and sediment concentration not as "continuous" but as "binary", the eight distribution maps in Figure 4 can be interpreted as representing conditional probabilities of f_2 for adimentional density under the conditions Equation 7:

$$f_2 = \left(\sigma^* \middle| \begin{pmatrix} t = 30, 90 \\ d = d_{Large}, d_{Small} \\ c = c_{still}, c_{slurry} \end{pmatrix} \right) \tag{7}$$

where, t: time [s], d: the diameter of pumices [mm], and d_{Large}, d_{Small} is the average particle sizes for the Large/Small groups of pumices used in this study. Additionally, c: the volumetric sediment concentration in the fluid, c_{still}, c_{slurry} corresponds to sediment concentrations under the Still/Slurry water. The same interpretation can be applied even to Figure 6, which can be considered as the conditional probability derived from the experimental setup for this study. This suggests that determining f_1 and f_2 through experimental sampling allows for the formulation of the water infiltration of pumice, ultimately providing a statistical model equipped with a wide range of interdisciplinary parameters. In this contribution, the experiments and results are based on the samples from a limited particle size ranges (<5.8 cm) and a specific research area (Ena pumice derived from the Eniwa Volcano in Atsuma, Hokkaido). However, the research including

this study, suggest that the water absorption property of pumice vary depending on its size and internal structure (e.g. Mitchell *et al.*, 2024).

Therefore, further research using pumice with different sizes and internal structures that reflect various eruption processes may be necessary. Also, the investigation was limited to fixed sediment concentration, c, and particle size, ϕ ($c = \frac{5}{400}, \phi < 125$ µm) while a significant difference in the data variability was observed between still and slurry conditions. Future research is required to clarify the effect of different concentration and particle size on water infiltration of pumice

4. Conclusion

Thus, the results of the laboratory experiment implied that the density of pumiceous materials could vary depending on time and size (1.164, 1.1271 g/cm^3 with 30 seconds; 1.186, 1.1468 g/cm^3 with 90 seconds, for small/large samples, respectively). Also, the behaviour has the potential to influence the behaviour of pumice rafts, illustrating the necessity of the current model improvement according to the density variation due to the water infiltration, taking it into an account that the behaviour and the data dispersion could vary with size and even whether or not they are immersed into the condition filled with particles (according to the experimental results, p-value of F test was at a minimum of 0.00851 be-tween small and large samples in slurry). Additionally, the results of the distribution sug-gest the possibility of a cross-disciplinary statistical model for pumice behaviours.

Acknowledgements

In this research, we are grateful for the assistance of anonymous reviewers and the editors for their invaluable comments to improve this paper.

Author Contributions

Conceptualization: Sho, S., Christopher, G.; **methodology**: Sho, S., Christopher, G., Takashi, K.; **investigation**: Sho, S.; **writing—original draft preparation**: Sho, S.; **writing—review and editing**: Sho, S., Christopher, G., Takashi, K.; **visualization**: Sho, S. All authors have read and agreed to the published version of the manuscript.

Conflict of interest

All authors declare that they have no conflicts of interest.

Data availability

Data is available upon reasonable request.

Funding

This research received no external funding.

References

Bryan, S. E., Cook, A., Evans, J. P., Colls, P. W., Wells, M. G., Lawrence, M. G., Jell, J. S., Greig, A., & Leslie, R. (2004). Pumice rafting and faunal dispersion during 2001–2002 in the Southwest Pacific: Record of a dacitic submarine explosive eruption from Tonga. *Earth and Planetary Science Letters*, 227(1–2), 135–154. doi: 10.1016/j.epsl.2004.08.009

Bryan, W. B. (1968). Low-potash dacite drift pumice from the Coral Sea. *Geological Magazine*, 105(5), 431–439. doi: 10.1017/S0016756800054819

Casadevall, T.J. (1993). *Volcanic Hazards and Aviation Safety: Lessons of the Past Decade*. Flight Safety Digest.

Christmann, C., Nunes, R.R., Schmitt, A.R., & Guffanti, M. (2017). *Flying into Volcanic Ash Clouds: An Evaluation of Hazard Potential.* The North Atlantic Treaty Organization, Vilnius, Lithuania.

Fiske, R. S., Cashman, K. V., Shibata, A., & Watanabe, K. (1998). Tephra dispersal from Myojinsho, Japan, during its shallow submarine eruption of 1952-1953. *Bulletin of Volcanology*, 59(4), 262–275. doi: 10.1007/s004450050190

Global Volcanism Program. (2024). [Database] Volcanoes of the World (v. 5.2.4; 21 Oct 2024). Distributed by Smithsonian Institution, compiled by Venzke, E. doi: 10.5479/si.GVP.VOTW5-2024.5.2

Gudmundsson F, Ingolfsson A (1967) Goose barnacles (Lepas spp.) on Surtsey pumice. *Náttúrufraedingurinn*, 37, 57-60.

Jokiel, P. L., & Cox, E. F. (2003). Drift pumice at Christmas Island and Hawaii: Evidence of oceanic dispersal patterns. *Marine Geology*, 202(3–4), 121–133. doi: 10.1016/S0025-3227(03)00288-3

Jutzeler, M., Marsh, R., Carey, R. J., White, J. D. L., Talling, P. J., & Karlstrom, L. (2014). On the fate of pumice rafts formed during the 2012 Havre submarine eruption. *Nature Communications*, 5(1), 3660. doi: 10.1038/ncomms4660

Maeno, F., Kaneko, T., Ichihara, M., Suzuki, Y., Yasuda, A., Nishida, K., & Ohminato, T. (2022). *First timeseries record of a large-scale silicic shallow-sea phreatomagmatic eruption*. Retrieved From https://www.researchsquare.com/article/rs-1272855/v1

Majcen, A., Gohla, J., Steinhoff, A. S., Meißner, L., Tassoti, S., & Spitzer, P. (2024). Fractionating microplastics by density gradient centrifugation: A novel approach using LuerLock syringes in a low-cost density gradient maker. *Chemistry Teacher International*, 6(3), 259–267. doi: 10.1515/cti-2023-0079

Manville, V., Segschneider, B., & White, J. D. L. (2002). Hydrodynamic behaviour of Taupo 1800a pumice: Implications for the sedimentology of remobilized pyroclasts. *Sedimentology*, 49(5), 955–976. doi: 10.1046/j.1365-3091.2002.00485.x

Manville, V., White, J. D. L., Houghton, B. F., & Wilson, C. J. N. (1998). The saturation behaviour of pumice and some sedimentological implications. *Sedimentary Geology*, 119(1–2), 5–16. doi: 10.1016/S0037-0738(98)00057-8

Murch, A. P., White, J. D. L., Barreyre, T., Carey, R. J., Mundana, R., & Ikegami, F. (2020). Volcaniclastic Dispersal During Submarine Lava Effusion: The 2012 Eruption of Havre Volcano, Kermadec Arc, New Zealand. *Frontiers in Earth Science*, 8, 237. doi: 10.3389/feart.2020.00237

Murch, A. P., White, J. D. L., & Carey, R. J. (2019). Characteristics and Deposit Stratigraphy of Submarine-Erupted Silicic Ash, Havre Volcano, Kermadec Arc, New Zealand. *Frontiers in Earth Science*, 7, 1. doi: 10.3389/feart.2019.00001

Nagayama A., & Izaki T. (2022). The Experiments Of Pumice Stone Drifting Of The Moving Process In The Wind Tunnel. Journal of Japan Society of Civil Engineers, Ser. *B3 (Ocean Engineering)*, 78(2), I_865-I_870. doi: 10.2208/jscejoe.78.2_I_865

Ohno, Y., Iguchi, A., Ijima, M., Yasumoto, K., & Suzuki, A. (2022). Coastal ecological impacts from pumice rafts. *Scientific Reports*, 12(1), 11187. doi: 10.1038/s41598-022-14614-y

Oppenheimer, C. (2003). Climatic, environmental and human consequences of the largest known historic eruption: Tam bora volcano (Indonesia) 1815. *Progress in Physical Geography: Earth and Environment*, 27(2), 230–259. doi: 10.1191/0309133303pp379ra

Orosa, P., Pasandín, A. R., & Pérez, I. (2021). Compaction and volumetric analysis of cold in-place recycled asphalt mixtures prepared using gyratory, static, and impact procedures. *Construction and Building Materials*, 296, 123620. doi: 10.1016/j.conbuildmat.2021.123620

Pradit, S., Puttapreecha, R., Noppradit, P., Buranapratheprat, A., & Sompongchaiyakul, P. (2022). The first evidence of microplastic presence in pumice stone along the coast of Thailand: A preliminary study. *Frontiers in Marine Science*, 9, 961729. doi: 10.3389/fmars.2022.961729

Prata, A.J., & Rose, W.I. (2015). Volcanic Ash Hazards to Aviation. *The Encyclopedia of Volcanoes (Second Edition)*, 911-934. doi: 10.1016/B978-0-12-385938-9.00052-3

Reagan, M. K., Turner, S., Legg, M., Sims, K. W. W., & Hards, V. L. (2008). 238U- and 232Th-decay series constraints on the timescales of crystal fractionation to produce the phonolite erupted in 2004 near Tristan da Cunha, South Atlantic Ocean. *Geochimica et Cosmochimica Acta*, 72(17), 4367–4378. doi: 10.1016/j.gca.2008.06.002

Redick, N. R. (2023). Review of Pumice Raft Formation Environments, Saturation, and Dispersal Mechanisms. *McGill Science Undergraduate Research Journal*, 18(1), B19–B25. doi: 10.26443/msurj.v18i1.187

Richards, A. F. (1958). Transpacific distribution of floating pumice from Isla San Benedicto, Mexico. *Deep Sea Research* (1953), 5(1), 29–35. doi: 10.1016/S0146-6291(58)80005-3

Risso, C., Scasso, R. A., & Aparicio, A. (2002). Presence of large pumice blocks on Tierra del Fuego and South Shetland Islands shorelines, from 1962 South Sandwich Islands eruption. *Marine Geology*, 186(3–4), 413–422. doi: 10.1016/S0025-3227(02)00190-1

Sutherland, F. L. (1965). Dispersal of Pumice, Supposedly from the 1962 South Sandwich Islands Eruption, on Southern Australian Shores. *Nature*, 207(5004), 1332–1335. doi: 10.1038/2071332a0

Vaughan, R. G., Abrams, M. J., Hook, S. J., & Pieri, D. C. (2007). Satellite observations of new volcanic island in Tonga. *Eos, Transactions American Geophysical Union*, 88(4), 37–41. doi: 10.1029/2007EO040002

Von Lichtan, I. J., White, J. D. L., Manville, V., & Ohneiser, C. (2016). Giant rafted pumice blocks from the most recent eruption of Taupo volcano, New Zealand: Insights from palaeomagnetic and textural data. *Journal of Volcanology and Geothermal Research*, 318, 73–88. doi: 10.1016/j.jvolgeores.2016.04.003

Whitham, A.G. and Sparks R.S.J. (1986). Pumice, Bull Volcanol. *Springer Nature Link*, 48, 209-223.

Witham, C., Webster, H.N., Hort, M.C., Jones, A., & Thomson, D.J. (2012). Modelling concentrations of volcanic ash encountered by aircraft in past eruptions. *Atmospheric Environment*, 48, 219-229.

Woodroffe, C. D., & Stancheva, M. (2024). Sustaining Coastal and Marine environments in the Anthropocene: Guest editors. *Journal of Coastal Conservation*, 28(3), 51. doi: 10.1007/s11852-024-01051-4

Yeo, I. A., McIntosh, I. M., Bryan, S. E., Tani, K., Dunbabin, M., Dobson, K. J., Mitchell, S. J., Collins, P. C., Clare, M. A., Cathey, H., Duwai, I., Brandl, P. A., Stone, K., & Manu, M. S. (2024). The 2019 pumice raft forming eruption of Volcano-F (Volcano 0403–091) and implications for hazards posed by submerged calderas. *Journal of Volcanology and Geothermal Research*, 454, 108160. doi: 10.1016/j.jvolgeores.2024.108160

Yin, Q., Gong, P., & Wang, X. (2024). Potential role of microplastic in sediment as an indicator of Anthropocene. *Earth Critical Zone*, 1(1), 100016. doi: 10.1016/j.ecz.2024.100016

Yoshida, K., Tamura, Y., Sato, T., Sangmanee, C., Puttapreecha, R., Ono, S. (2022) Petrographic characteristics in the pumice clast deposited along the Gulf of Thailand, drifted from Fukutoku-Oka-no-Ba. *Geochem. J.*, 56, 134–137.

Yoshida, K., Tamura, Y., Sato, T.,Hanyu, T., Usui, Y., Chang, Q., & Ono, S. (2022). Variety of thedrift pumice clasts from the 2021 Fukutoku-Oka-no-Baeruption, Japan. *Island Arc*, 31(1), e12441. doi: 10.1111/iar.12441

Yu S., Yang L., Junhua X., Pengxiang Z., Shugang L. (2023). Study on particles sedimentation in porous media with the immersed boundary-lattice Boltzmann flux solver. *Computers & Mathematics with Applications*, *129*, 1–10. doi: 10.1016/j.camwa.2022.11.012

Zhang X., Huang T., Ge Z., Man T., Huppert E. H. (2025). Infiltration characteristics of slurries in porous media based on the coupled Lattice-Boltzmann discrete element method, *Computers and Geotechnics*, 177, 1–18. doi: 10.1016/j.compgeo.2024.106865